Supplementary data for:

Functional characterisation of a *PBX1 de novo* missense variant identified in a patient with syndromic congenital heart disease

Dimuthu Alankarage [1], Justin Szot [1], Nick Pachter [2,3], Anne Slavotinek [4,5], Licia Selleri [5,6], Joseph Shieh [4,5], David Winlaw [1,7,8], Eleni Giannoulatou [1,9], Gavin Chapman [1, 9], Sally L. Dunwoodie [1,9 *]

[1] Victor Chang Cardiac Research Institute, Darlinghurst, Sydney, Australia; [2] Genetic Services of Western Australia, King Edward Memorial Hospital, Perth, Australia; [3] University of Western Australia, Perth, Australia; [4] Division of Medical Genetics, Department of Pediatrics, University of California San Francisco, CA, USA; [5] Institute of Human Genetics, University of California San Francisco, CA, USA; [6] Program in Craniofacial Biology, Department of Orofacial Sciences and Department of Anatomy, University of California San Francisco, CA, USA; [7] Heart Centre for Children, The Children's Hospital at Westmead, Sydney, Australia; [8] Faculty of Medicine and Health, University of Sydney, Sydney, Australia; [9] Faculty of Medicine, University of New South Wales, Sydney, Australia.

Corresponding author

* Corresponding author: Tel: +61 2 9295 8613, E-mail: s.dunwoodie@victorchang.edu.au

Supplementary tables

Supplementary table 1: Rare, damaging variants that segregate with disease in family 3467.

INHERITANCE MODEL	***De novo***		**Compound heterozygous**	
Gene name	*PBX1*	*ESPNL*	*OBSCN*	*ATRN*
Chromosome	CHR1	CHR2	CHR1	CHR20
Genomic position†	164768976	239039979	228503767; 228520630	3565467; 3578621
Variant type	Non-synonymous	Non-synonymous	Non-synonymous; non-synonymous	Non-synonymous; non-synonymous
DNA variant change	551G>C	2624G>A	16103G>A; 18593A>G	3124C>T; 3538A>G
Amino acid change	R184P	R875Q	R5368Q; Y6198C	L1042F; I1180V
gnomAD Heterozygotes # (MAF)	0 (0)	3 (0.00001453)	13 (0.00005698); 14 (0.00004999)	0 (0); 8 (0.00003186)
gnomAD Homozygotes #	0	0	0; 0	0; 0
CADD-PHRED	33	19.98	29.8; 28	22.1; 27.4
PolyPhen2-HVAR (prediction)	0.995 (probably damaging)	0.997 (probably damaging)	0.976 (probably damaging); 0.999 (probably damaging)	0.992 (probably damaging); 0.978 (probably damaging)

As the proband has sporadic CHD, variants that were *de novo*, recessive and compound heterozygous were considered. They were filtered by minor allele frequency (<0.01) and by predicted pathogenicity by CADD-PHRED (≥15) and Polyphen-HVAR (≥0.446). Two *de novo* variants in genes *PBX1* and *ESPNL* as well as compound heterozygous variants in *OBSCN* and *ATRN* were identified. †Relative to hg19. MAF: Minor Allele Frequency, with respect to gnomAD. PolyPhen2-HVAR: 0 (benign) – 1 (probably damaging). CADD-PHRED: 1-99; ≥10 (top 10% of deleterious mutation); ≥20 (top 1% of deleterious mutation).

Supplementary table 2. Phenotype details of patients reported with pathogenic, single gene *PBX1* variants. Patients with missense variants are presented first, followed by patients with loss-of-function alleles.

	Missense						
		Slavotinek, 2017[a]					Eozenou, 2019[b]
Amino acid position	**R184P[c]**	**M224K**	**R227P**	**R234P**	**R235Q**	**R235Q**	**R235Q**
CHD	TOF with absent pulmonary valve	PDA, ASD		PDA, pulmonary artery hypertension	PDA		
Renal/ Urinary	Increased renal echogenicity			Increased renal cortical echogenicity, mild left pyelocaliectasis	Bilateral dilated ureters		
Reproductive		DSD (microphallus, prepuce-like opening, splayed labioscrotal appearance, intra-abdominal testicular tissue, persistent mullerian ducts)	Bilateral cryptorchidism		Small scrotum, bilateral cryptorchidism	Micropenis, cryptorchid right gonad, absent left gonad, uterine didelpys, labial folds with no palpable gonads, 2 perineal openings, vaginal introitus, urethral meatus	Female external genitalia, streak gonads (right gonad, sparse seminiferous tubules, fibrous tissue; left gonad, fibrous tissue), bilateral Fallopian tubes and epididymal structures
Skeletal	Mild clinodactyly						Radiocubital synostosis
Respiratory	Bronchiolitis	Pulmonary hypertension, chronic respiratory failure		Chronic lung disease, pulmonary aspiration	Right lung hypoplasia, right eventration of the diaphragm, persistent pulmonary hypertension		

Digestive		Feeding intolerance, oral motor dysfunction, gastroesophageal reflux disease, pancreatic insufficiency		Gastrointestinal reflux disease, dysphagia			
Craniofacial	Broad nasal tip, thick lips, prominent philtrum, anteverted ears	Esotropia (left eye)	Strabismus, sacral dimple		Blue sclera, ear microtia, prominent nuchal folds, micrognathia		
Nervous system	Autism	Hypoplasia of corpus callosum, parenchymal volume loss, diffuse hypotonia, dysautonomia		Hypotonia		Cortical hyperintensity, cerebellar microhaemorrhages, mild subdural hematoma	
Growth/size/body		Global developmental delay	Gross motor delay	Global developmental delay			
Other[d]		Thromobocytopenia	Hemangioma		Nail bed hypoplasia, nuchal cystic hygroma		
Sex	Male	Male	Male	Female	Male	Male	Male

	LOF								
	Riedhammer, 2017[e]	**Heidet, 2017[f]**		**Slavotinek, 2017[a]**		**Le Tanno, 2017[g]**		**Heidet, 2017[f]**	
Amino acid position	**G138Vfs*40**	**N143Tfs*37**	**R184***	**S262Qfs*2**	**R288***	**1.5Mb deletion (only *PBX1*)**	**0.276 MB deletion (only *PBX1*)**	**Deletion of one *PBX1* allele**	**Deletion of one *PBX1* allele**
CHD					Ebstein anomaly				
Renal/ Urinary	Small hyperechogenic kidneys	Renal hypoplasia	Hyperechogenic kidneys with cysts	Renal hypoplasia, increased renal cortex echogenicity, malrotated right kidney	Hypoplastic kidneys, urinary tract infections	Bilateral renal hypoplasia, hyperechogenicity	Bilateral renal hypoplasia, right renal ectopia, right renal dysplasia	Small dysplastic horseshoe kidney	Single hyperechogenic kidney
Reproductive	Bilateral cryptorchidism			Small labia minora		Bilateral cryptorchidism	Right cryptorchidism		
Skeletal	Short clavicles, bilateral clinodactyly	Scoliosis			Mild brachydactyly, slender fingers and toes	Shoulder blade anomaly, acromioclavicular joint, skull basis, vertebral defects, hip dislocation	Joint laxity		
Respiratory					Upper airway infections				
Digestive				Type 1 choledochal cyst	Constipation				

Craniofacial	Wide nasal bridge, short neck, bilateral over folding of the helix	Deafness	Long narrow face	Hearing loss, microtia, hypoplastic ear helices with bilateral absence of tragus, attached earlobes, stenosis of external auditory canals, wide lateral eyebrows, upslanted palpebral fissures, epicanthal folds, flat nasal bridge, thin philtrum, narrow palate, small jaw	Low anterior and posterior hairlines, coarse hair, deep-set eyes, a short philtrum, an exaggerated cupid's bow, bifid uvula, posteriorly rotated ears with attached earlobes and small external auditory canals, a prominent mandible, a sacral dimple, genu valgum	Bilateral ear dysplasia, divergent strabismus, short nose, anteverted nares, prominent philtrum, short neck	Bilateral conductive hearing loss, bilateral ear dysplasia	Deafness	Microcephaly, facial dysmorphism (long narrow face, abnormal ear lobes)
Nervous system				Mild truncal and axial hypotonia	Autism	Hypotonia			
Growth/size/body	Global developmental delay		Developmental delay, growth retardation	Mild motor delay	Truncal obesity with slender extremities, delayed psychomotor development	Motor delay	Global developmental delay, global motor delay, autism spectrum disorder		Developmental delay
Other[d]				Asymmetric gluteal cleft	Otitis media, pes planovalgus (flat feet)				
Sex	Male	Female	Female	Female	Female	Male	Male	Female	Male

([a]Slavotinek et al., 2017 (1), [b]Eozenou et al., 2019 (2), [c]Current manuscript, [e]Riedhammer et al., 2017 (3), [f]Heidet et al., 2017 (4), [g]Le Tanno et al., 2017 (5)). [d]Other include phenotypes that do not fall within any other category.

Supplementary figures

A

```
PBX1_HUMAN MDEQPRLMHSHAGVGMAGHPGLSQHLQDGAGGTEGEGGRKQDIGDILQQIMTITDQSLDE 60
PBX1_MOUSE MDEQPRLMHSHAGVGMAGHPGLSQHLQDGAGGTEGEGGRKQDIGDILQQIMTITDQSLDE 60
           ************************************************************

PBX1_HUMAN AQARKHALNCHRMKPALFNVLCEIKEKTVLSIRGAQEEEPTDPQLMRLDNMLLAEGVAGP 120
PBX1_MOUSE AQARKHALNCHRMKPALFNVLCEIKEKTVLSIRGAQEEEPTDPQLMRLDNMLLAEGVAGP 120
           ************************************************************

PBX1_HUMAN EKGGGSAAAAAAAAASGGAGSDNSVEHSDYRAKLSQIRQIYHTELEKYEQACNEFTTHVM 180
PBX1_MOUSE EKGGGSAAAAAAAAASGGAGSDNSVEHSDYRAKLSQIRQIYHTELEKYEQACNEFTTHVM 180
           ************************************************************

PBX1_HUMAN NLLREQSRTRPISPKEIERMVSIIHRKFSSIQMQLKQSTCEAVMILRSRFLDARRKRRNF 240
PBX1_MOUSE NLLREQSRTRPISPKEIERMVSIIHRKFSSIQMQLKQSTCEAVMILRSRFLDARRKRRNF 240
           ****************************************************************

PBX1_HUMAN NKQATEILNEYFYSHLSNPYPSEEAKEELAKKCGITVSQVSNWFGNKRIRYKKNIGKFQE 300
PBX1_MOUSE NKQATEILNEYFYSHLSNPYPSEEAKEELAKKCGITVSQVSNWFGNKRIRYKKNIGKFQE 300
           ************************************************************

PBX1_HUMAN EANIYAAKTAVTATNVSAHGSQANSPSTPNSAGSSSSFNMSNSGDLFMSVQSLNGDSYQG 360
PBX1_MOUSE EANIYAAKTAVTATNVSAHGSQANSPSTPNSAGSSSSFNMSNSGDLFMSVQSLNGDSYQG 360
           ************************************************************

PBX1_HUMAN AQVGANVQSQVDTLRHVISQTGGYSDGLAASQMYSPQGISANGGWQDATTPSSVTSPTEG 420
PBX1_MOUSE AQVGANVQSQVDTLRHVISQTGGYSDGLAASQMYSPQGISANGGWQDATTPSSVTSPTEG 420
           ************************************************************

PBX1_HUMAN PGSVHSDTSN 430
PBX1_MOUSE PGSVHSDTSN 430
           **********
```

B

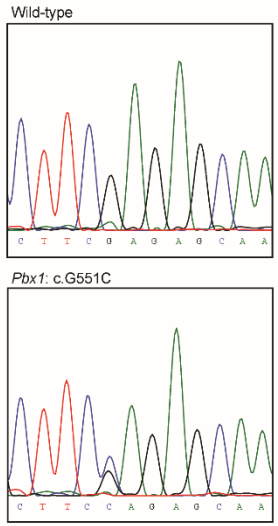

Supplementary figure 1. (A) Amino acid sequence conservation between human and mouse PBX1. The 430 amino acid protein is completely conserved between the two species. Residue R184 is indicated in *red*. (B) Sanger sequencing of the founder PBX1-R184P mouse created by Crispr-Cas9. Nucleotide change *Pbx1*:c.551G>C is observed in the founder and not present in wild-type, unaltered mice.

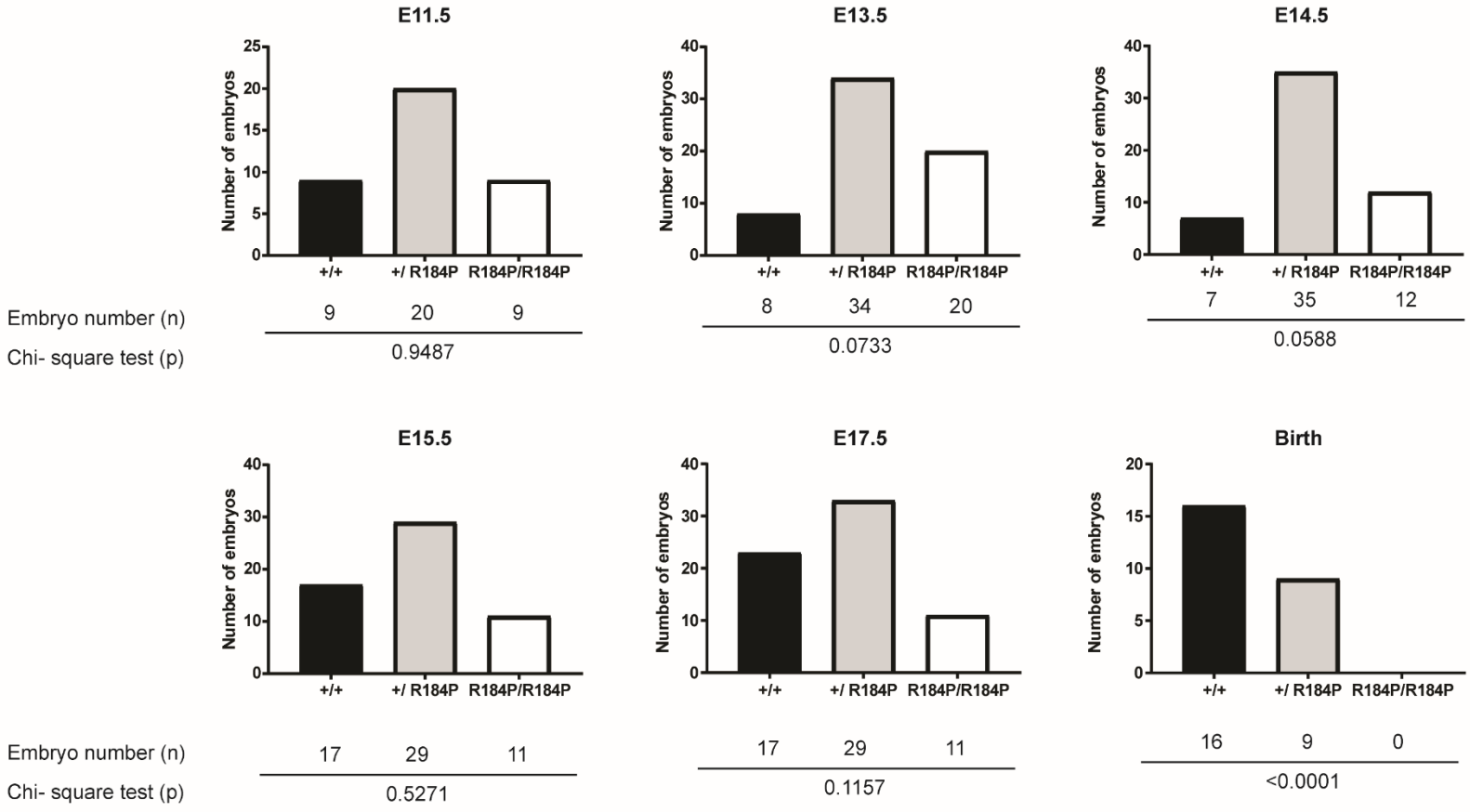

Supplementary figure 2. Mendelian ratios observed in embryos derived from matings between heterozygous males and heterozygous females at six stages of development (E11.5, E13.5, E14.5, E15.5, E17.5 and birth). Chi-square test was performed to detect deviations from expected versus observed numbers of embryos for wild-type (+/+), heterozygous (+/R184P) and homozygous (R184P/R184P) genotypes.

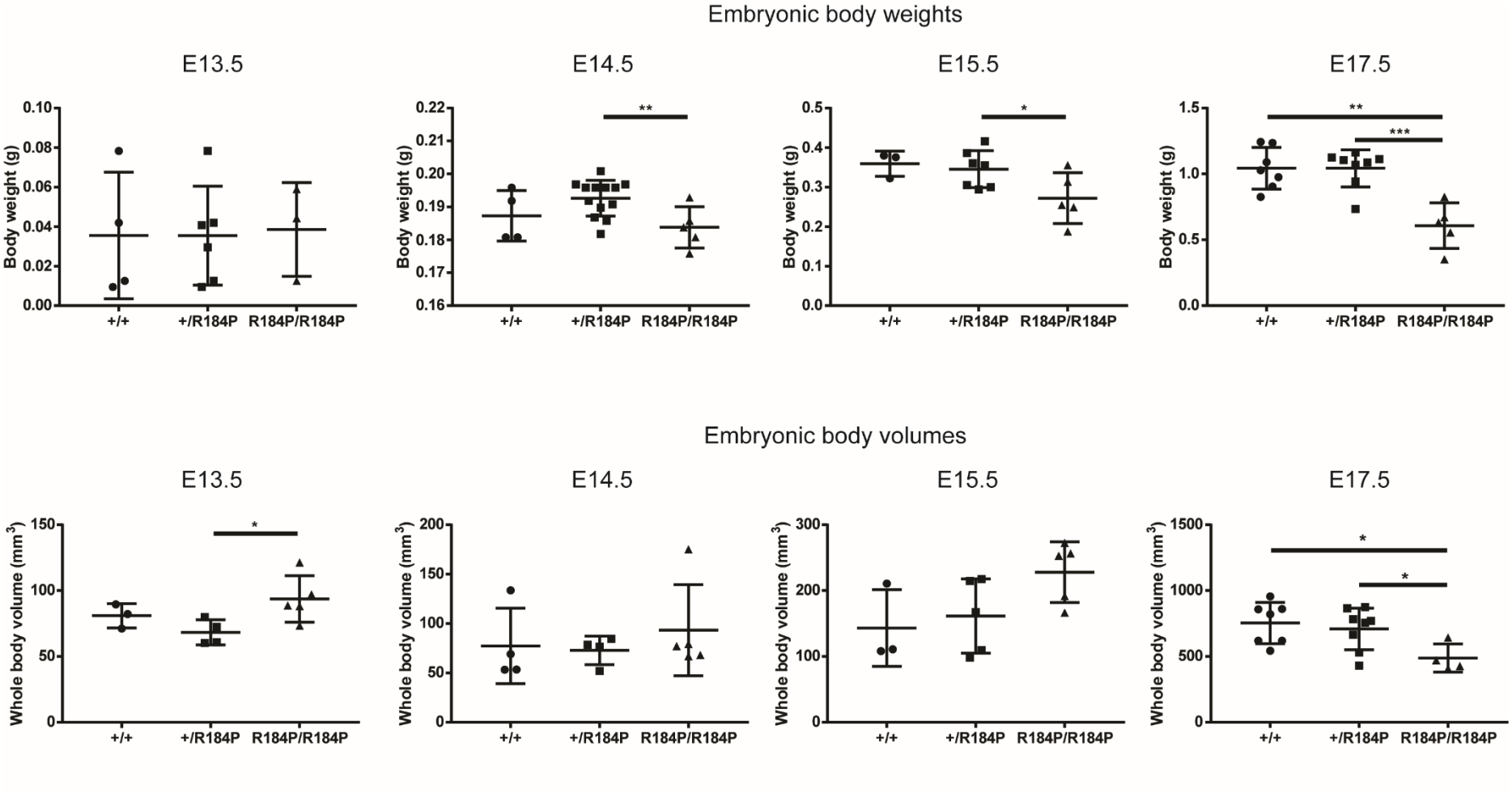

Supplementary figure 3. Embryonic body weights and body volumes of the wild-type, heterozygous and homozygous embryos at four stages of development (E13.5, E14.5, E15.5 and E17.5). (n ≥ 12 per stage, * p <0.05, ** p <0.01, *** p <0.001)

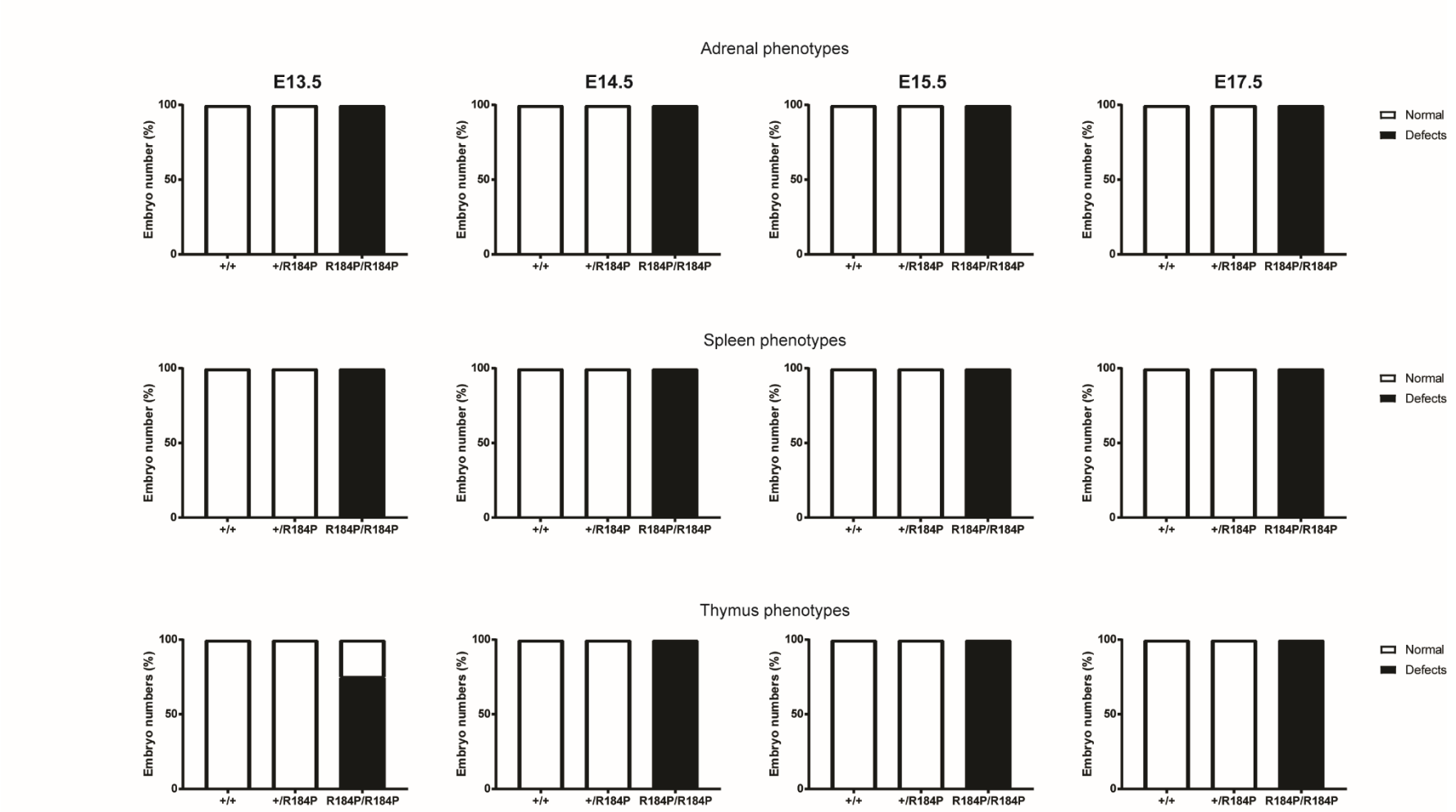

Supplementary figure 4. R184P/R184P homozygous embryos exhibited abnormal adrenal glands, spleen and thymi. Adrenal glands and spleen were aplastic. Thymi were absent or ectopic. Defects in these organs were not observed in wild-type or heterozygous embryos. (n ≥ 15 per stage).

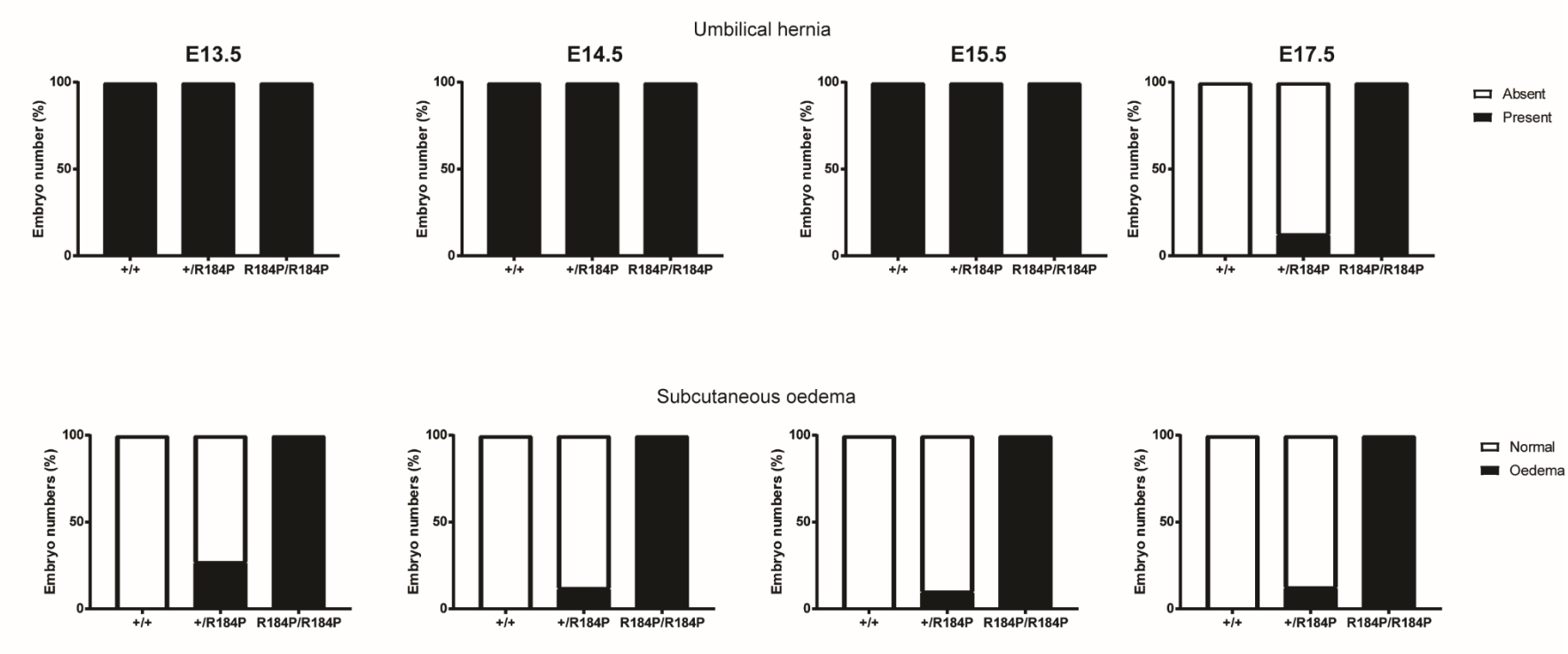

Supplementary figure 5. Umbilical hernia was observed in wild-type, heterozygous and homozygous embryos at E13.5, E14.5 and E15.5. At E17.5, wild-type embryos no longer exhibited umbilical hernia. 12.5% of heterozygous embryos had umbilical hernia. All homozygous embryos continued to exhibit umbilical hernia. Subcutaneous oedema was observed in 27% of heterozygous embryos at E13.5, 12% at E14.5, 10% at E15.5, and 12.5% at E17.5. All homozygous embryos displayed subcutaneous oedema at all stages analysed. This phenotype was not observed in any wild-type embryos analysed. (n ≥ 15 per stage).

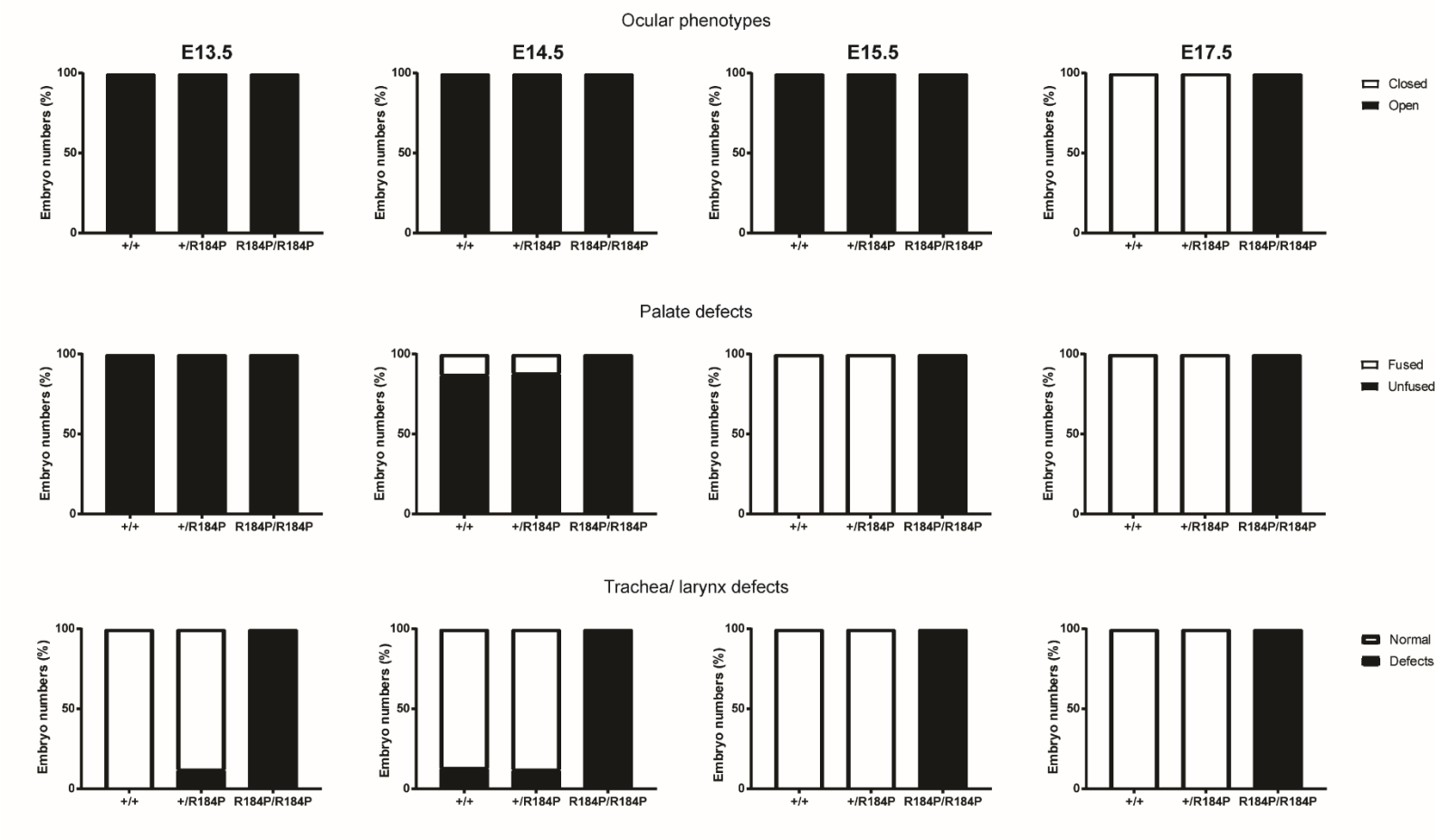

Supplementary figure 6. Eyes stay open in wild-type, heterozygous and homozygous embryos at E13.5, E14.5 and E15.5. At E17.5, wild-type and heterozygous embryos have closed eyes. At this stage, the homozygous embryos continue to display open eyes. At E13.5, all wild-type, heterozygous and homozygous embryos had unfused secondary palatal shelves. At E14.5, 13% of wild-type and 12% of heterozygous embryos had fused palatal shelves. At E15.5 and at E17.5, all wild-type and heterozygous embryos had fused palatal shelves. Homozygous embryos at these stages continued to exhibit unfused palatal shelves. In homozygous embryos, trachea were atretic at all stages. The larynx

was atretic until E17.5. In heterozygous embryos, 12% had atretic larynx at E13.5 and E14.5, and were normal at E15.5 and E17.5. Atretic larynx were observed in 13% of wild-type embryos at E14.5 and at no other stages. (n ≥ 14 per stage).

References

1 Slavotinek, A., Risolino, M., Losa, M., Cho, M.T., Monaghan, K.G., Schneidman-Duhovny, D., Parisotto, S., Herkert, J.C., Stegmann, A.P.A., Miller, K. *et al.* (2017) De novo, deleterious sequence variants that alter the transcriptional activity of the homeoprotein PBX1 are associated with intellectual disability and pleiotropic developmental defects. *Human molecular genetics*, **26**, 4849-4860.
2 Eozenou, C., Bashamboo, A., Bignon-Topalovic, J., Merel, T., Zwermann, O., Lourenco, D., Lottmann, H., Lichtenauer, U., Rojo, S., Beuschlein, F. *et al.* (2019) The TALE homeodomain of PBX1 is involved in human primary testis-determination. *Human mutation*, in press.
3 Riedhammer, K.M., Siegel, C., Alhaddad, B., Montoya, C., Kovacs-Nagy, R., Wagner, M., Meitinger, T. and Hoefele, J. (2017) Identification of a Novel Heterozygous De Novo 7-bp Frameshift Deletion in PBX1 by Whole-Exome Sequencing Causing a Multi-Organ Syndrome Including Bilateral Dysplastic Kidneys and Hypoplastic Clavicles. *Frontiers in pediatrics*, **5**, 251.
4 Heidet, L., Moriniere, V., Henry, C., De Tomasi, L., Reilly, M.L., Humbert, C., Alibeu, O., Fourrage, C., Bole-Feysot, C., Nitschke, P. *et al.* (2017) Targeted Exome Sequencing Identifies PBX1 as Involved in Monogenic Congenital Anomalies of the Kidney and Urinary Tract. *Journal of the American Society of Nephrology : JASN*, **28**, 2901-2914.
5 Le Tanno, P., Breton, J., Bidart, M., Satre, V., Harbuz, R., Ray, P.F., Bosson, C., Dieterich, K., Jaillard, S., Odent, S. *et al.* (2017) PBX1 haploinsufficiency leads to syndromic congenital anomalies of the kidney and urinary tract (CAKUT) in humans. *Journal of medical genetics*, **54**, 502-510.